JPn Neuroscience

The Journal of Physiology

J Physiol 592.1 (2014) pp 171–188

Diversity of vestibular nuclei neurons targeted by cerebellar nodulus inhibition

Hui Meng[1], Pablo M. Blázquez[2], J. David Dickman[1] and Dora E. Angelaki[1]

[1] *Department of Neuroscience, Baylor College of Medicine, Houston, TX 77030, USA*
[2] *Department of Otolaryngology, Washington University School of Medicine, St Louis, MO, USA*

Key points

- Electrical stimulation of the cerebellar nodulus and ventral uvula decreases the time constant of the horizontal vestibulo-ocular reflex during yaw rotation.
- Unlike the flocculus and ventral paraflocculus which target a particular cell group, nodulus/ventral uvula inhibition targets a large diversity of cell types in the vestibular nuclei.
- Twenty per cent of nodulus/ventral uvula-target neurons were sensitive to both vestibular stimuli and eye movements, whereas the majority was only sensitive to vestibular stimuli.
- Most nodulus/ventral uvula-target cells responded to both rotation and translation and only approximately half discriminated translational and gravitational accelerations.
- Projections of the nodulus/ventral uvula to both eye movement-and non-eye movement-sensitive vestibular nuclei neurons suggest a role in both eye movement generation and vestibulo-spinal or thalamo-cortical systems.

Abstract A functional role of the cerebellar nodulus and ventral uvula (lobules X and IXc,d of the vermis) for vestibular processing has been strongly suggested by direct reciprocal connections with the vestibular nuclei, as well as direct vestibular afferent inputs as mossy fibres. Here we have explored the types of neurons in the macaque vestibular nuclei targeted by nodulus/ventral uvula inhibition using orthodromic identification from the caudal vermis. We found that all nodulus-target neurons are tuned to vestibular stimuli, and most are insensitive to eye movements. Such non-eye-movement neurons are thought to project to vestibulo-spinal and/or thalamo-cortical pathways. Less than 20% of nodulus-target neurons were sensitive to eye movements, suggesting that the caudal vermis can also directly influence vestibulo-ocular pathways. In general, response properties of nodulus-target neurons were diverse, spanning the whole continuum previously described in the vestibular nuclei. Most nodulus-target cells responded to both rotation and translation stimuli and only a few were selectively tuned to translation motion only. Other neurons were sensitive to net linear acceleration, similar to otolith afferents. These results demonstrate that, unlike the flocculus and ventral paraflocculus which target a particular cell group, nodulus/ventral uvula inhibition targets a large diversity of cell types in the vestibular nuclei, consistent with a broad functional significance contributing to vestibulo-ocular, vestibulo-thalamic and vestibulo-spinal pathways.

(Received 31 May 2013; accepted after revision 7 October 2013; first published online 14 October 2013)
Corresponding author D. Angelaki: Department of Neuroscience, Baylor College of Medicine, One Baylor Plaza, Houston, TX 77030, USA. Email: dangelaki@cns.bcm.edu

DOI: 10.1113/jphysiol.2013.259614

Abbreviations 2D/3D, two-/three-dimensional; BT, burst-tonic; EH, eye–head; EM, eye movement; FB, front–back; FL, flocculus and ventral paraflocculus; FN, fastigial nuclei; FR, Fourier ratio; FTN, flocculus target neuron; GA, gravitational acceleration; GIA, gravitoinertial acceleration; IFR, instantaneous firing rate; LR, left–right; NU, nodulus and ventral uvula; PVP, position-vestibular-pause; VN, vestibular nuclei; VOR, vestibulo-ocular reflex.

Introduction

The vestibulo-cerebellum consists of the flocculus and ventral paraflocculus (FL), which are involved in vestibulo-ocular plasticity and smooth pursuit eye movements (Boyden *et al.* 2004; Ilg & Thier, 2008; Lisberger, 2009, 2010; Broussard *et al.* 2011; Gao *et al.* 2012), as well as the nodulus (lobule X) and ventral uvula (lobule IXc,d) (NU), which are thought to be involved in spatial orientation (Wearne *et al.* 1997; Cohen *et al.* 1999; Barmack, 2003; Angelaki *et al.* 2010). The FL has been extensively studied, whereas the neurophysiology of the NU remains poorly understood. Lesions of the NU result in severe spatial disorientation, postural instability, spontaneous nystagmus, vomiting, and large deficits in both the dynamics and the spatial organization of the vestibulo-ocular reflex (VOR) (Angelaki & Hess, 1994*b*; 1995*a*,*b*; Wearne *et al.* 1998; Wiest *et al.* 1999; Walker *et al.* 2008, 2010; Rota *et al.* 2012). These effects indicate that the NU has a major role in vestibular function. Not surprisingly, the NU receives major mossy fibre inputs from vestibular afferents and the vestibular nuclei, with large reciprocal connections to the latter (Brodal & Brodal, 1985; Epema *et al.* 1985; Thunnissen *et al.* 1989; Ono *et al.* 2000). NU Purkinje cells respond to tilt and translation stimuli, reflecting both vertical canal and otolith system contributions (Marini *et al.* 1975, 1976; Precht *et al.* 1976; Barmack & Shojaku, 1995; Fushiki & Barmack, 1997; Barmack & Yakhnitsa, 2002, 2003; Yakhnitsa & Barmack, 2006; Yakusheva *et al.* 2007, 2008, 2010).

Recent studies (Yakusheva *et al.* 2007; Laurens *et al.* 2013*a*,*b*) have also suggested that the NU is involved in solving an important sensory ambiguity of otolith afferents, which encode gravitoinertial acceleration (GIA) and respond identically to both inertial motion (translation) and changes in orientation relative to gravity (tilt) (Angelaki *et al.* 2004; Dickman *et al.* 1991; Fernandez *et al.* 1972). According to theory, an internal estimate of orientation relative to gravity (GA) can be inferred by 'combining' otolith and semicircular canal information, as well as prior knowledge about the statistics of commonly experienced linear accelerations (Merfeld, 1995; Zupan *et al.* 2002; Green & Angelaki, 2004, 2007; Green *et al.* 2005; Laurens & Droulez, 2007; Laurens & Angelaki, 2011; Laurens *et al.* 2013*a*,*b*). Second, given this GA estimate, translational acceleration (TA) can be computed by simple subtraction: TA = GA – GIA. In fact, Yakusheva *et al.* (2007, 2008, 2010) and Laurens *et al.* (2013*a*,*b*) have reported that NU Purkinje cells carry convergent otolith and semicircular canal signals that allow them to respond selectively to either translational motion or tilt, whereas GIA-coding cells are few in the NU. In contrast, a mixed representation of translation, tilt and GIA signals has been found in the VN (Angelaki *et al.* 2004; Green *et al.* 2005; Shaikh *et al.* 2005; Zhou *et al.* 2006).

To understand the role of the NU in vestibular processing, it is important to discern which vestibular nuclei (VN) neurons receive NU projections and their modulatory properties. Based on previous lesion studies producing VOR deficits (Angelaki & Hess, 1995*a*,*b*; Wearne *et al.* 1998; Walker *et al.* 2008, 2010), we hypothesize that some NU-target VN neurons are sensitive to eye movements and are involved in VOR control. In addition, given the postural and disorientation deficits following NU lesions, we also expect some NU-target neurons will be correlated with the ability to discriminate tilt from translation. It is possible, for example, that cells encoding translation or tilt will receive NU signals, while VN cells encoding GIA will not. The goal of the present study is to identify NU-target neurons and characterize their properties to eye movements, rotation, translation and combination stimuli. Results show that NU-target neurons have a wide range of properties, consistent with a broad functional significance.

Methods

Animals and experimental set-up

Three juvenile monkeys (*Macacca mulatta*) were chronically implanted with a delrin ring to restrain head movements during experiments. A recording platform with predrilled holes spaced 0.8 mm apart was secured stereotaxically within the head-restraining ring via dental cement. The predrilled holes on the recording platform were orientated at an angle of 10 deg medio-laterally (from both the left and the right sides), thereby allowing electrode penetrations to reach the medial portion of the NU while avoiding the sagittal sinus. Search coils were also chronically implanted for measuring eye movements (for details see Angelaki *et al.* 2000, 2001; Meng *et al.* 2005). The surgical and experimental procedures conformed to the National Institutes of Health guidelines and the principles of UK regulations and were approved by the Institutional Animal Care and Use Committee.

Head-restrained animals were seated comfortably in a primate chair that was mounted inside a vestibular turntable (Acutronics, Pittsburgh, PA, USA). The turntable delivered rotations in three dimensions (yaw, pitch and roll) and translations along any direction in

the earth-horizontal plane. The animal's position on the turntable was adjusted such that (1) the rotation axes passed through the centre of the head (i.e. the intersection of the sagittal plane with the interaural line), and (2) the horizontal stereotaxic plane was parallel to the earth-horizontal plane.

To elicit saccadic and pursuit eye movements, a visual target (red dot) was back-projected onto a screen placed 46 cm away from the animal using a laser and *x–y* mirror galvanometers (GSI Lumonics, Moorpark, CA, USA). We monitored the animal's motion using the output of a three-dimensional accelerometer that was mounted on the inner frame of the turntable, as well as velocity and position signals from the rotators. These signals, as well as eye coil voltages, were filtered (200 Hz, 6 pole Bessel), digitized at a rate of 833.33 Hz and stored for off-line analysis. Stimulus delivery and data acquisition were controlled with custom written scripts for the Spike2 software environment via a Cambridge Electronics Design (CED, Cambridge, UK) data acquisition interface (model Power 1401, 16 bit resolution). Eye movement calibration procedures were similar to those used in previous studies (Meng *et al.* 2005; Meng & Angelaki, 2006).

Criteria for appropriate placement of stimulating electrodes in the nodulus

Using stereotaxic coordinates, as well as the abducens nuclei, the fourth ventricle and the VN as landmarks, the NU was first mapped based on strong translation responsiveness of both simple and complex spikes (Yakusheva *et al.* 2007, 2008, 2010). Once the boundaries of the NU were identified using high impedance electrodes, low impedance tungsten microelectrodes (0.1–0.5 MΩ impedance; FHC, Bowdoinham, ME, USA) were used to electrically stimulate the cerebellar cortex. These low impedance electrodes were not adequate to record single cell activity, but they could record multiunit activity and complex spikes, as well as identify the fourth ventricle (no activity). Appropriate placement of stimulation electrodes was guided by stimulation-evoked effects on eye movements (Solomon & Cohen, 1994). Specifically, short trains (4–5 s) of electrical pulses applied to the nodulus and ventral uvula decrease the horizontal VOR time constant during constant velocity yaw rotation in darkness, but elicit no nystagmus in the absence of head rotation. On the other hand, electrical stimulation of the dorsal uvula does not affect the horizontal VOR time constant but produces nystagmus with a rapid rise in eye velocity (Heinen *et al.* 1992; Solomon & Cohen, 1994).

Thus, to determine appropriate placement of each stimulating electrode, we delivered 4 s electrical pulse trains while the animal was passively rotating about the yaw axis at a constant velocity of 60 deg/s. The pulse trains were composed of biphasic pulses 0.4 ms in duration (0.2 ms of positive phase followed by 0.2 ms of negative phase), 3 ms inter-pulse intervals (333 Hz) and a constant current amplitude of 100 μA. Identical pulse trains were delivered 1 s after the onset and offset of rotation in all experiments. Electrical stimulation was repeated every 500 μm while lowering the electrode into the NU. When the most effective site was identified, the electrode was anchored in place. In early recordings, multiple stimulating electrodes were employed simultaneously and kept fixed in their effective locations for several days. However, stimulation effects on VOR time constant weakened or even vanished within a few days after electrode placement. Therefore, in later recordings (which comprise most of the data here), only one monopolar electrode was implanted daily and removed at the end of the experiment. This ensured that all data reported here were collected while the stimulating electrode was appropriately placed within the NU.

Neural recordings

Extracellular recordings from isolated single neurons in the VN were obtained with epoxy-coated tungsten microelectrodes (4–6 MΩ impedance; FHC). Two electrodes were introduced into the brain daily: a high impedance electrode was directed towards the VN, and a low impedance stimulating electrode was placed in the NU (see above). Each electrode reached the brainstem/cerebellum through a 26 gauge cannula and was manipulated with a remote-controlled microdrive (FHC). The action potentials were discriminated online using a dual time-amplitude window discriminator (BAK, Germantown, MD, USA) and used to trigger acceptance pulses that were stored on a PC through the event channel of the CED Power 1401. Neural activity was amplified, filtered (300 Hz–6 kHz), digitized at a rate of 25 kHz and stored for offline spike sorting (if online isolation was suboptimal).

We explored a large area $10 \times 4 \times 4$ mm lateral and posterior to the abducens nucleus, but NU-target VN neurons were recorded within a $6 \times 3 \times 3$ mm area (Fig. 1, blue/red filled symbols). A search stimulus consisting of rotation, translation and/or pursuit was utilized as the electrode was lowered into the brainstem/cerebellum. Upon isolation, each VN neuron was first tested for orthodromic connectivity with the NU. Biphasic pulses (1–3 Hz) of 0.4 ms duration and 100–400 μA amplitude (at least 100 pulses) were delivered to the NU stimulating electrode. An active Wiener filter (Artifact Zapper, Riverbend Instruments, Birmingham, AL, USA) that dynamically reduces stimulation artifact was used for enhancing spike isolation (Paul & Gnadt, 2003). NU-target neurons were identified online by their inhibitory responses in the

peristimulus time histogram (similar to previous studies: Zhang *et al.* 1993, 1995; Lisberger *et al.* 1994).

As the same current intensity of up to 400 μA was applied to all sites, variation in inhibition duration and latency was probably due to different connection strengths and the characteristics of the pathway connecting the stimulation site with the recorded neuron. For example, neurons receiving direct inhibition from the stimulated site should present short latency of inhibition, but neurons that are inhibited from other sites in the NU, which are activated indirectly (e.g. through parallel fibres), would have longer latency. The NU is a large structure that spans several millimetres, so it is not surprising that such an indirect activation will be present in a large portion of the neurons. It is also possible that some cells identified as NU-target neurons with long latencies are connected indirectly with the NU through other VN neurons (see Discussion).

Once an NU-target cell was identified as described above, it was next characterized as non-eye-movement (non-EM), PVP (position-vestibular-pause), EH (eye-head) or BT (burst-tonic), based on responses during static fixation, horizontal/vertical smooth pursuit (0.5 Hz, $\pm$10 deg) and 0.5 Hz ($\pm$10 deg) yaw/pitch oscillations during fixation of a central head-fixed target ('VOR suppression', as in previous studies; Angelaki *et al.* 2001; Meng *et al.* 2005; Meng & Angelaki, 2006; Green *et al.* 2007).

Upon successful classification, neurons were further tested using 0.5 Hz sinusoidal translation (lateral and fore-aft; 0.5 Hz $\pm$0.2 g, where $g = 9.8$ m/s^2), followed by combined tilt and translational stimuli along the best-responding direction in complete darkness. These stimuli were identical to those used previously to independently manipulate inertial and gravitoinertial accelerations (Angelaki *et al.* 2004; Shaikh *et al.* 2005; Meng *et al.* 2007; Yakusheva *et al.* 2007). They consisted of pure translation (translation), pure tilt (tilt) or combined translation and tilt (tilt minus translation and tilt plus translation). The tilt stimulus consisted of a 0.5 Hz sinusoidal rotation from an upright position with peak amplitude of 11.3 deg (peak velocity of 36 deg/s). As this motion reorientates the head relative to gravity, otolith afferents are stimulated by a linear acceleration component in the horizontal plane with a peak magnitude of 0.2g. The amplitude of the translation stimulus was adjusted to match that induced by the head tilt ($\pm$20 cm). During combined rotational and translational stimulation, the inertial and gravitational acceleration components combine in either an additive or a subtractive manner, depending on the relative directions of the two stimuli. As a result, the net GIA in the horizontal plane either doubles (tilt plus translation) or becomes nearly zero (tilt minus translation), although the actual translational component remains the same. By comparing cell responses under these conditions, one can ascertain whether the cell responds selectively to translational motion alone, to tilt alone or, like primary otolith afferents, to net GIA (Angelaki *et al.* 1999, 2004).

Data analysis

Data analysis was performed offline using Matlab (MathWorks, Natick, MA, USA). Eye position was calibrated, as described in detail elsewhere (Angelaki, 1998; Angelaki *et al.* 2000). Positive directions of horizontal and vertical eye movements were leftward and downward, respectively. Saccades and fast phases of nystagmus were identified and removed through a semi-automated computer algorithm based on a higher derivative of eye velocity (Angelaki, 1998; Angelaki & Hess, 1994*a*,*b*). The algorithm offered manual inspection of the automatically detected fast phases and allowed the experimenter to correct potential misidentifications. Slow phase eye velocity was calculated to estimate VOR response amplitude and time constant of decay for the horizontal eye velocity component during constant velocity yaw rotation. Time constants were determined empirically by measuring the time interval in which the amplitude of slow phase eye velocity fell to 1/e (37%) of its peak value. By comparing the VOR time constants without and with electrical stimulation of the NU, effective nodulus stimulation sites were recognized only when a decrease of at least 30% in time constant was observed (Fig. 1, open blue and orange symbols).

Two types of analyses were performed. First, to compute gain and phase, instantaneous firing rates (IFRs) from at least 10 response cycles were folded into a single cycle and fitted by a sinusoidal function (for details see Meng *et al.* 2005; Meng & Angelaki, 2006). Response amplitude refers to half the peak-to-trough modulation. Neural response gain for rotation was computed as the ratio between response amplitude and peak stimulus velocity (in units of spikes per second per degree per second). Response phase for rotation was calculated as the difference between peak neural response and peak head angular velocity. Response gain and phase of NU-target neurons during translation were expressed relative to linear acceleration.

In addition, a permutation analysis was used to determine whether a cell modulated significantly during each stimulus. Cumulative IFRs were binned into 40 bins per cycle and a Fourier ratio (FR) was defined as the fundamental frequency divided by the maximum of any of the first 20 harmonics. Then the 40 bins were shuffled randomly to remove any modulation and a FR was calculated again. The randomization process was repeated 1000 times and if the original FR was higher than the FRs of 99% of the permuted data, the modulation was considered to be significant ($P < 0.01$). Classification of NU-target cells as non-EM (i.e. no significant modulation

during both horizontal and vertical smooth pursuit eye movements), PVP (significant modulation during both pursuit and rotational VOR suppression), EH (significant modulation during both pursuit and rotational VOR suppression) or BT (significant modulation during pursuit, but not during rotational VOR suppression) was based on this analysis. PVP and EH cells were distinguished based on response phase during pursuit and rotation stimuli (see Meng *et al.* 2005 for details).

For cells whose responses were recorded during at least two motion directions, their spatiotemporal tuning was quantified by fitting a two-dimensional (2D) spatiotemporal model that uses the response gain and phase to two orthogonal directions to describe the neuron's tuning (Angelaki, 1991; Angelaki & Dickman, 2000). The 2D spatiotemporal model represents a generalization of cosine tuning that allows for both gain and phase to depend on stimulus direction (Angelaki, 1991; Bush *et al.* 1993; Angelaki & Dickman, 2000). Hence, we computed the maximum response gain and phase, as well as the corresponding preferred direction for each cell. The departure from cosine tuning is captured by the 'tuning ratio', ranging between 0 and 1, as the ratio of the minimum over the maximum neural response gain.

A second (correlation) analysis was used to distinguish whether a given neuron's response correlates best with tilt, translation or GIA, as follows (Laurens *et al.* 2013*b*). First, neuronal activity was expressed as spike density, using a 50 ms standard deviation Gaussian kernel. A cycle-by-cycle analysis was then performed to compute the neuronal gain and phase for each cycle, which created the neuron's response matrix X_{obs}, matched to the stimulus matrix $S = [s_p,\ s_r,\ s_{FB}$ and $s_{LR}]$, for pitch (s_p), roll (s_r), front–back (FB, s_{FB}) and left–right (LR, s_{LR}) acceleration components, respectively (expressed in units of g, $g = 9.81\ m\ s^{-2}$). The most general ('composite') model assumes $X_{obs} \approx H_{comp}.S' \approx h_p \times s_p + h_r \times s_r + h_{FB} \times s_{FB} + h_{LR} \times s_{LR}$, where h_p, h_r, h_{FB} and h_{LR} represent the neuron's response (gain and phase) to pitch tilt, roll tilt, FB and LR accelerations and are computed using multiple linear regression analysis.

In addition to the composite model, which assumes no a priori relationship between the four parameters, three 1st-order models were also considered: (i) a 'translation' model assumes that the neuron responds to translation only, and that its modulation during tilt should be 0, i.e. $h_p = h_r = 0$; (ii) a 'net gravito-inertial acceleration (GIA)' model assumes that $h_p = h_{FB}$ and $h_r = h_{LR}$; (iii) a 'tilt' model assumes that the neuron responds to tilt only, and that its modulation during translation should be 0, i.e. $h_{FB} = h_{LR} = 0$.

We classified VN cells as tilt-selective, translation-selective or GIA-selective by quantifying whether one of the 1st-order models fitted the cell's activity significantly better than the others using a bootstrap procedure (1000 samples, $P = 0.05$). Only translation-selective and GIA-selective NU-target cells were encountered; no tilt-selective NU-target cells were found (see Results). If no 1st-order model fitted the cell's responses significantly better than the others, then the cell was classified as composite.

This analysis gave identical classification results to the method used previously to distinguish translation- and GIA-selective cells (Angelaki *et al.* 2004; Yakusheva *et al.* 2007), but had the additional advantage that it also evaluated a third, tilt-selective, model (Laurens *et al.* 2013*b*). Given that none of the recorded NU-target neurons was classified as tilt-selective, and for a direct comparison with previous publications (Angelaki *et al.* 2004; Meng *et al.* 2007), we have repeated the Angelaki *et al.* (2004) analysis, as follows. We first computed partial correlation coefficients that describe how well each neuron's responses to the stimulus set could be predicted by the GIA or translation model. Subsequently, Fisher's r-to-z transform was used to normalize the variances of partial correlation coefficients. Scatter plots of z-scored partial correlation coefficients were then created and the difference in z-scores compared with inhibition latency.

Results

Behavioural effects of NU electrical stimulation during VOR

As shown in Fig. 2, electrical stimulation of the nodulus and lobule d of the uvula (collectively referred to here as 'NU') decreased the horizontal VOR time constant during yaw rotation, similar to the findings of Solomon & Cohen (1994). For the example in Fig. 2, the stimulating electrode was located in the left NU, approximately 3.5 mm from the midline. Without NU stimulation, the horizontal VOR time constant during rightward yaw rotation (60 deg/s) was 38.5 s (Fig. 2*A* – grey traces). During NU stimulation, the time constant dropped to 20.8 s 1 s after rotation onset (see Methods, Fig. 2*A* – black traces). In contrast, NU stimulation in isolation produced no nystagmus when delivered while the animal was seated motionless in the dark (Fig. 2*B*). These NU stimulation-evoked eye movements contrast with the responses evoked during stimulation of the dorsal uvula (Fig. 2*C* and *D*), which resulted in horizontal nystagmus both during rotation and while the animal was stationary. In addition, stimulation of the dorsal uvula did not change the VOR time constant (39.8 s *vs.* 40.5 s; see also Solomon & Cohen, 1994).

Summary data showing horizontal VOR time constants with (ordinate) and without (abscissa) stimulation from multiple sites in three animals is shown in Fig. 3. Blue and orange symbols represent sites for which NU stimulation shortened the horizontal VOR time constant during either rightward or leftward yaw rotations (pairs of points

connected with lines), but did not evoke nystagmus with the animal stationary in darkness (<10 deg/s; as with the example in Fig. 2*A* and *B*). According to Solomon & Cohen (1994), sites where stimulation produces no nystagmus on its own but changes the time constant of the horizontal VOR are found rostrally, in the nodulus and in sub-lobule d of the uvula, and our data are in agreement with theirs. Green symbols are used for four posterior sites (see Fig. 1), where electrical stimulation elicited horizontal nystagmus with a rapid onset and offset without changes in VOR time constant (as with the example of Fig. 2*C* and *D*). Sites where stimulation elicited nystagmus, without an effect on the VOR time constant, are presumably located in sub-lobules a and b of the dorsal uvula (Heinen *et al.* 1992; Solomon & Cohen, 1994). Finally, neither VOR time constant changes nor stimulation-evoked nystagmus was seen from stimulation of another 21 sites (Figs 1 and 3, black open symbols).

In the present experiments we were interested in characterizing VN cells receiving inhibition from the nodulus and/or sub-lobule d of the ventral uvula, because these areas are thought to be directly involved in controlling the 3D properties of the vestibular system (Angelaki & Hess, 1994*a*,*b*, 1995*a*,*b*; Solomon & Cohen, 1994; Wearne *et al.* 1998). Thus, VN recordings were restricted to days/sites with clear stimulation-induced effects on the horizontal VOR time constant. A total of 31 NU-target VN neurons (Fig. 1, filled blue and red symbols; animal D: $n = 22$; animal P: $n = 4$; animal H: $n = 5$) were recorded during 19 of these sessions with clear reduction in the horizontal VOR time constant (Figs 1 and 3, open blue symbols). Another 15 sites with notable reduction in horizontal VOR time constant were identified (Figs 1 and 3; open orange symbols), although no electrophysiologically identified NU-target cell was found on these sessions. VOR time constant effects were typically larger during ipsilateral rotation (relative to the stimulation site, 17/22; see also Solomon & Cohen, 1994).

Effects of NU stimulation on spontaneous activity of NU-target neurons

As illustrated in Fig. 4*A*, electrical stimulation of the NU site resulting in the behavioural effects shown in Fig. 2*A* inhibited the spontaneous activity of the example NU-target cell. Inhibition latency and duration were quantified from the raw data, using at least 100 repetitions of 100 ms traces aligned on the stimulus artifact (Fig. 4*A*). Inhibition latency was quantified as the time of the last spike (asterisk) before pause onset (Fig. 4*A*, inset, period B). Measurement of inhibition latency was confounded by the stimulus artifact that in most cases lasted up to 1 ms, and thus we could not measure latencies smaller than 1 ms. Inhibition duration was measured as the length of the silent period (Fig. 4*A*, inset, period C; defined between the two asterisks). Inhibition latency and duration for the example NU-target cell in Fig. 4*A* were B = 3.1 ms and C = 8.8 ms, respectively.

Of 31 identified NU-target neurons, inhibition latency ranged from 1 to 4.3 ms with a median of 3.04 ms (Fig. 4*B*). Inhibition duration varied from 3.9 ms to 15.8 ms (median: 7.9 ms; Fig. 4*C*). Although the

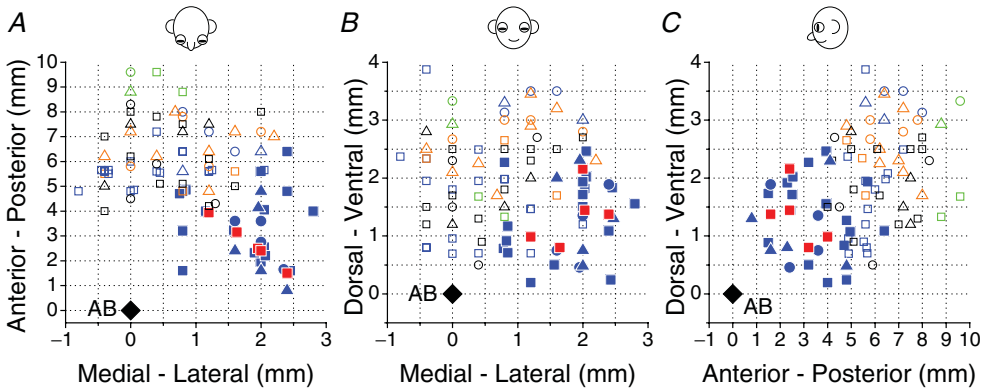

Figure 1. Reconstruction of NU stimulation sites and locations of 31 NU-target VN neurons
Top (*A*), frontal (*B*) and sagittal (*C*) views showing both NU stimulation sites (open symbols) and NU-target neurons (filled symbols) relative to the abducens nucleus (AB, black diamonds). Note that sites on the left (negative medial–lateral locations beyond 1 mm from midline) were flipped relative to the midline and plotted together with sites on the right (positive medial–lateral locations). Open blue and orange symbols represent NU stimulation sites, which shortened the horizontal VOR time constant ($n = 19$ and 15, respectively). Open green symbols show four posterior sites whose stimulation elicited nystagmus, without any change in the VOR time constant. Open black symbols represent stimulating sites without effects on the VOR time constant or nystagmus ($n = 21$). Filled blue symbols show the location of non-EM, NU-target neurons ($n = 26$), whereas filled red symbols illustrate five NU-target cells that were sensitive to eye movements. All 31 NU-target neurons were identified from stimulation of 19 NU sites with significant behavioural effects (open blue symbols). Different symbols represent neurons/sites from different animals.

same current intensity of 400 μA was applied to all sites, variation in inhibition duration and latency was probably due to different connection strengths and the characteristics of the specific pathways connecting the stimulation site with the recorded neuron (see Discussion). In 6 of the 31 identified NU-target neurons, the inhibition was followed by a transient increase in firing rate (rebound excitation; e.g. Fig. 4*A*). The remaining cells showed only inhibitory responses to NU stimulation.

Properties of NU-target neurons

Responses from a horizontal EH NU-target cell during 0.5 Hz horizontal smooth pursuit, yaw rotation, pitch rotation and lateral translation are illustrated in Fig. 5 (top traces). The neuron increased its firing rate during rightward (negative) eye movements (Fig. 5*A*) and rightward (negative) yaw rotation (VOR suppression; Fig. 5*B*), but did not modulate during either pitch rotation (Fig. 5*C*) or translation (Fig. 5*D*). Responses from a non-EM, NU-target cell are shown in Fig. 5 (bottom traces). That cell was insensitive to eye movements (Fig. 5*E*), but had clear modulation during sinusoidal yaw rotation (Fig. 5*F*) and lateral translation (Fig. 5*H*), as well as a weak response during pitch rotation (Fig. 5*G*).

All NU-target neurons were located ipsilateral to the stimulation site, but were scattered throughout the sampled area. Of the 31 NU-target neurons identified, only five were sensitive to eye movements (Fig. 1, filled red symbols), whereas the remaining 26 cells were non-EM neurons (Fig. 1, filled blue symbols). Of the five EM cells, three were PVPs (two preferred yaw rotation and one preferred vertical rotation) and two EH cells (both preferring yaw over vertical rotation). None of the EM cells responded significantly during either lateral or forward/backward translation while the animal suppressed its VOR by fixating a head-fixed target.

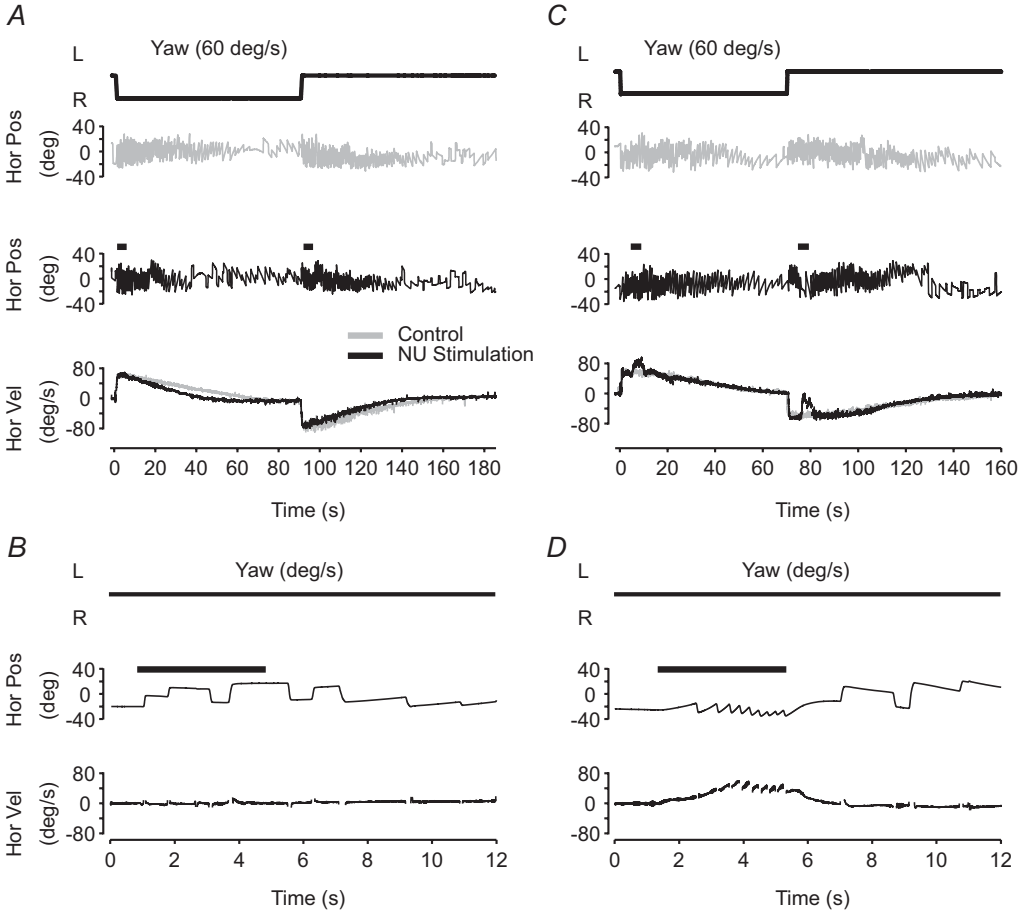

Figure 2. Examples of NU stimulation effects on eye movements
A and *C*, horizontal nystagmus ('Hor Pos') and slow phase eye velocity ('Hor Vel', bottom) induced by constant velocity yaw (rightward) rotation at 60 deg/s. Trials without (grey) and with (black) NU stimulation are illustrated. Short black bars in the middle panel indicate the timing and duration of stimulation (333 Hz, 100 μA, 4 s; see Methods). *B* and *D*, stimulation-induced eye movements with the animal upright and stationary in darkness. Data shown are from two different sites, corresponding to one blue (*A*, *B*) and one green (*C*, *D*) location in Fig. 1.

Translation responses were tested in darkness for 26 non-EM cells. Of these, 21 modulated significantly during lateral translation, 15 during forward/backward translation and 13 responded to both directions. In addition, more than half (15) significantly modulated during yaw rotation: 11 cells increased their firing during ipsilateral rotation (type I) and four during contralateral rotation (type II). The majority of these yaw-responding, non-EM, NU-target neurons responded significantly to translational motion (11/15) and/or pitch/roll rotation (9/15) as well. All cells that showed no modulation during yaw rotation (11) were sensitive to translational motion along either the lateral or the forward–backward axis, and 73% (8/11) modulated during both translation and pitch/roll rotation.

To ascertain whether NU-target neurons encode tilt, translation or net GIA, 23 non-EM cells were also tested during combinations of tilt and translation (Angelaki *et al.* 2004; Yakusheva *et al.* 2007). Figure 6 shows example responses during lateral translation, roll rotation (referred as 'tilt') and combination stimuli. Cell 1 responded similarly to translation and tilt. The response of this cell resembled that of otolith afferents, which selectively encode GIA, regardless of whether the stimulus arises from translation or tilt relative to gravity (Fernandez & Goldberg, 1976; Angelaki *et al.* 2004). In contrast, cell 2 showed a clear modulation during translation, but no significant modulation during roll tilt. In addition, the cell modulated similarly during tilt minus translation and tilt plus translation. Thus, this cell encodes translation and ignores changes in head orientation relative to gravity.

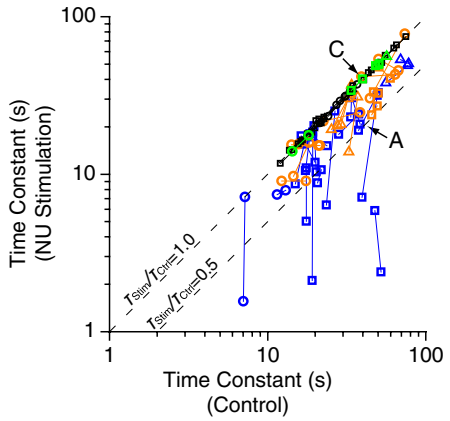

Figure 3. Summary of NU stimulation effects on eye movements
The scatter plot compares VOR time constant with (ordinate, 'NU Stimulation') and without (abscissa, 'Control') NU stimulation. Data points from the same stimulation site during leftward and rightward rotation are connected by lines. Blue ($n = 19$) and orange ($n = 15$) open symbols represent sites that did not elicit nystagmus, but resulted in a decrease in the horizontal VOR time constant during at least one direction of yaw rotation. Green open symbols ($n = 4$) represent sites where stimulation evoked nystagmus with the animal stationary (no vestibular stimulation). Black symbols ($n = 21$) represent NU stimulation sites without any effects on eye movements. All VN neurons driven by NU stimulating electrodes were obtained from the 19 sites shown in blue. Data points marked A and C represent the example VOR data shown in *A* and *C* of Fig. 2. Different symbols represent data from different animals. Dashed lines illustrate slopes of 1 and 0.5 (i.e. ratio of VOR time constants with and without stimulation, $T_{Stim}/T_{Ctrl} = 1$ or 0.5).

Figure 7 summarizes responses of 23 NU-target cells tested during tilt, translation and their combinations. Nine NU-target neurons were classified as GIA-coding cells and another 11 as translation-selective cells (Fig. 7, filled black and red symbols, respectively). GIA-selective neurons responded similarly to tilt and translation, with gains along the unity slope (dashed) line (e.g. Fig. 7*A*, black filled symbols). Translation-selective neurons had lower gains during tilt than during translation (Fig. 7*A*, red filled symbols). During tilt minus translation, translation-selective cells had responses that were similar to those during translation, whereas GIA-selective cells had attenuated responses (Fig. 7*B*). Finally, during tilt plus translation, only translation-selective cells had responses that were identical to those during translation (Fig. 7*C*, red filled symbols). In contrast, GIA-selective cell modulation was larger during tilt plus translation than during translation (Fig. 7*C*, black filled symbols). We did not identify any tilt-selective NU-target cells. Responses of three additional NU-target neurons did not fit either GIA or translation-coding models (Fig. 7*A–C*, grey filled symbols) and were classified as 'composite' (see Methods). Thus, in terms of tilt and translation responses, NU-target neurons also represent a continuum, covering the whole range of properties encountered in the VN (Angelaki *et al.* 2004).

Normalized partial correlation coefficients of the translation (TA) and GIA-tuned models are shown in Fig. 8*A*. There was no significant correlation between the difference in the two model *z*-scores and inhibition latency (Spearman rank correlation, $r = 0.18$, $P = 0.41$; Fig. 8*B*). As illustrated in Fig. 8*C*, inhibition duration and latency showed only a weak correlation (Spearman rank correlation, $r = 0.34$, $P = 0.09$). Both small and large latencies and durations were found for both TA- and GIA-selective cells.

Finally, responses at multiple directions were obtained for 17 NU-target, non-EM neurons during translation and 11 NU-target, non-EM cells during rotation. As illustrated in Fig. 8*D*, preferred directions and gains for NU-target neuron responses were broadly distributed, similar to the properties of a larger population of VN neurons described previously (Angelaki & Dickman, 2000; Dickman & Angelaki, 2002). Translational gains of NU-target cells along the maximum response direction ranged from 63.6 to 534.1 spikes/s/g (median = 256). Rotational gains ranged from 0.29 to 1.55 spikes s^{-1} deg^{-1} g^{-1} (median = 0.88). Tuning ratios for translation ranged

from 0.01 to 0.41 (median = 0.19), whereas tuning ratios for rotation ranged from 0.09 to 0.51 (median = 0.16). Thus, the subpopulation of VN cells targeted by NU inhibition covers the whole range of response properties described for large populations of VN neurons described in previous studies (Angelaki & Dickman, 2000; Dickman & Angelaki, 2002; Angelaki *et al.* 2004; Chen-Huang & Peterson, 2006, 2010; Zhou *et al.* 2006; Angelaki & Yakusheva, 2009; Marlinski & McCrea, 2009).

Discussion

Here we have characterized the response properties of VN neurons targeted by NU inhibition during eye movements and 3D vestibular stimuli. There are two main findings regarding the properties of NU-target neurons. First, unlike flocculus-target neurons (FL), which are exclusively of the EH type (Zhang *et al.* 1993, 1995; Lisberger *et al.* 1994), NU-target VN cells do not exhibit uniform and stereotyped properties. Most (84%) were non-EM cells and only five cells were sensitive to both vestibular stimulation and eye movements. None of the NU-target cells identified here was sensitive only to eye movements. Projections of the NU to both EM and non-EM VN neurons suggests a role in both eye movement generation and vestibulo-spinal or thalamo-cortical systems.

The second notable finding is the diversity of vestibular properties encountered in NU-target neurons. We have previously shown that most NU Purkinje cells respond selectively to either translation or tilt,

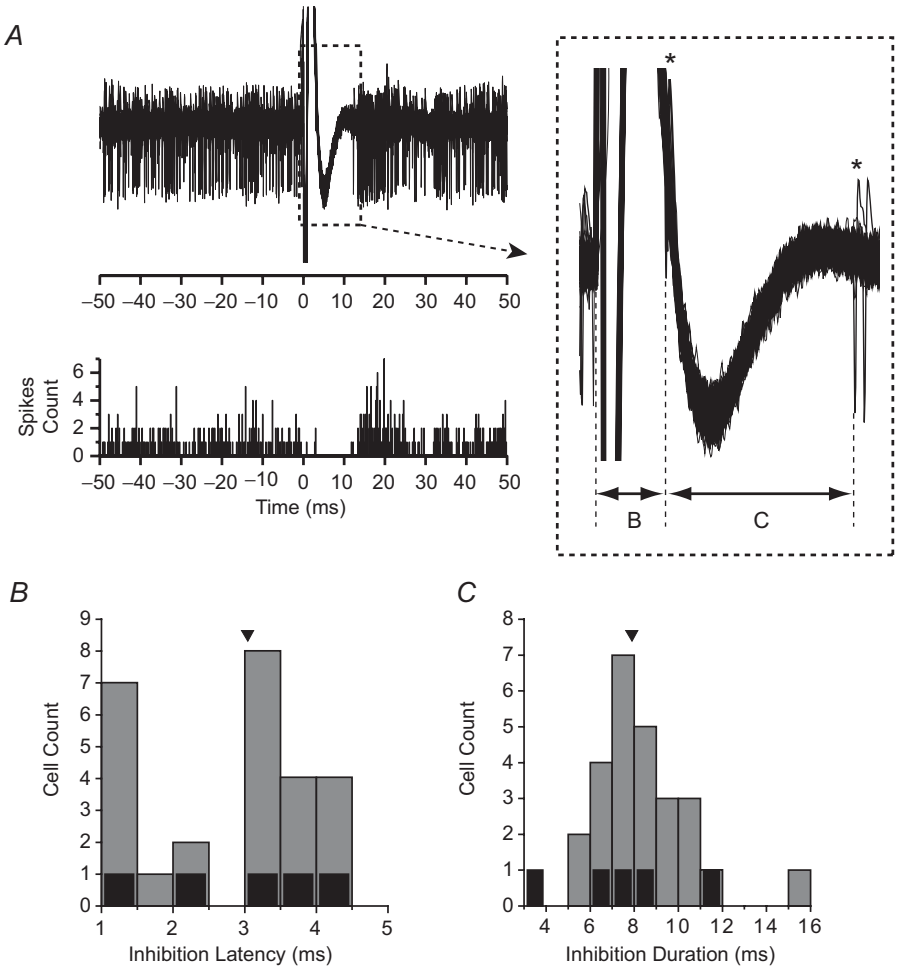

Figure 4. Inhibition latency and duration of NU-target neurons
A, top: stimulation-induced inhibition of the spontaneous activity of an example cell identified using the stimulating electrode whose behavioural effects are shown in Fig. 2*A* and *B*. In total, 140 trials were superimposed and aligned on the stimulation artifact onset (time = 0). Inset: enlargement of the traces in the dashed box, showing how inhibition latency and duration were defined. Asterisks (*) mark timing of action potentials used to define latency (*B*) and duration (*C*) of inhibition. Bottom: corresponding peristimulus time histogram (bin width = 0.2 ms). *B* and *C*, distributions of inhibition latency (*B*, arrowhead indicates median = 3.04 ms) and inhibition duration (*C*, arrowhead indicates median = 7.9 ms). Grey bars represent non-EM cells, while black bars represent five VN neurons with eye movement sensitivity.

and few to GIA (Yakusheva *et al.* 2007; Laurens *et al.* 2013*a*,*b*). In contrast, VN neurons show a broad continuum of properties: translation-selective, tilt-selective, GIA-selective and in-between responses (Angelaki *et al.* 2004; Zhou *et al.* 2006). Based on these findings, we suggested that a network connecting the NU and the VN might be responsible for disambiguation of the GIA and generation of translation and tilt encoding responses. Thus, we hypothesized that NU-target cells might be selective to translation or tilt, as with NU Purkinje cells (Laurens *et al.* 2013*a*,*b*). To address this hypothesis, we studied the responses of NU-target neurons during a tilt/translation protocol identical to that used in earlier studies (Angelaki *et al.* 2004; Shaikh *et al.* 2005; Yakusheva *et al.* 2007). Contrary to expectations, we found that NU-target neurons in the VN represent a continuum with some cells resembling vestibular afferents (GIA-selective), some translation coding neurons and others having a mixed response. These results suggest that NU-target neurons have a wide

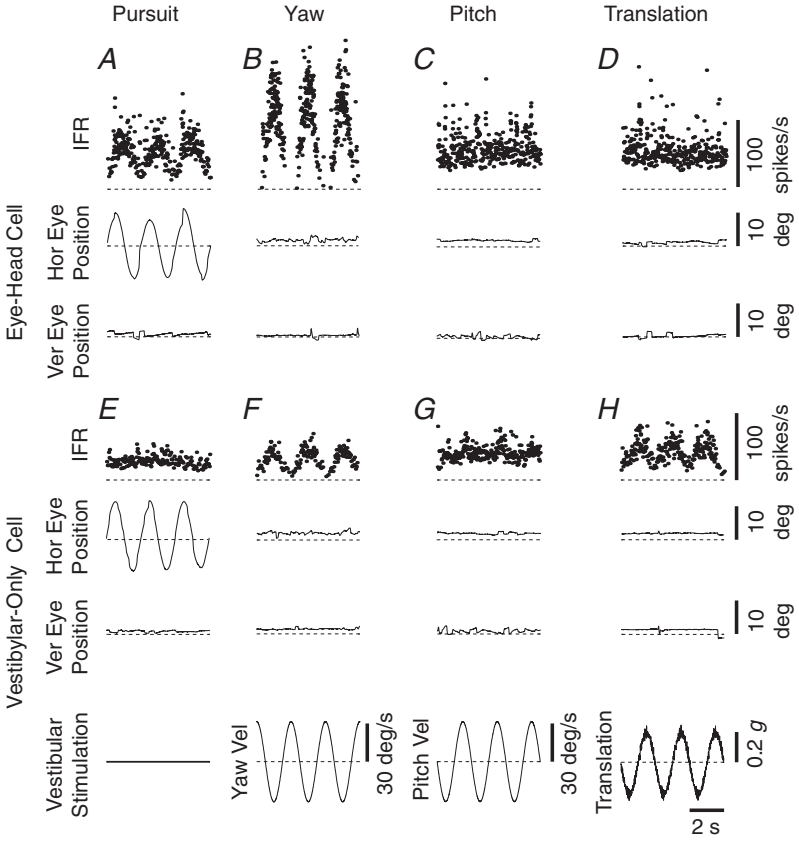

Figure 5. Example NU-target neuron responses
EH neuron (*A*–*D*) and non-EM neuron (*E*–*H*) responses during smooth pursuit eye movement (1st column), yaw rotation (2nd column), pitch rotation (3rd column) and lateral translation (4th column). Positive deflections indicate leftward eye movement, leftward yaw rotation, downward pitch rotation and leftward translation, respectively. Motion profiles are illustrated in the bottom row. Animals were required to fixate a head-fixed target (VOR suppression) during rotation and translation. IFR, instantaneous firing rate; Hor, horizontal; Ver, vertical; Vel, velocity; $g = 9.8$ m/s^2.

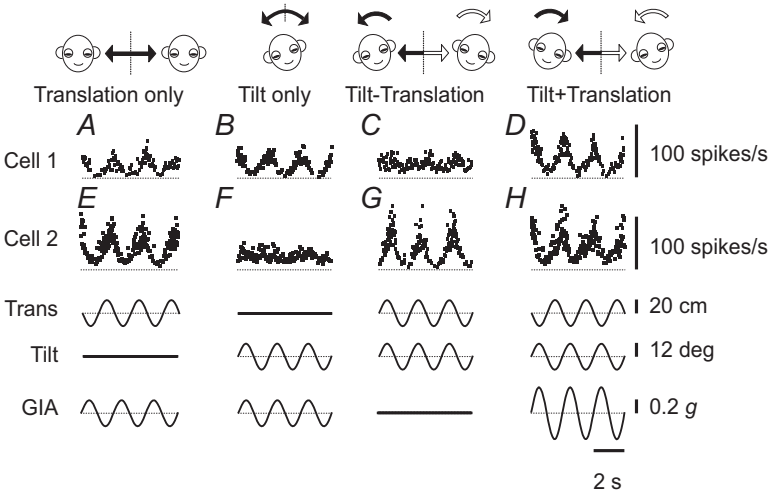

Figure 6. Example NU-target neuron responses during combinations of translation and tilt
Instantaneous firing rates of two example cells during translation (*A*), tilt (*B*), tilt-translation (*C*) and tilt+translation (0.5 Hz) (*D*). The translation and tilt stimuli (bottom traces) were matched in both amplitude and direction to elicit an identical net acceleration in the horizontal plane. Cell 1 (same cell as shown in Fig. 4*A*) encodes net gravitoinertial acceleration (GIA). Cell 2 selectively modulates during translation regardless of changes in head orientation relative to gravity (Tilt). Trans, translation; $g = 9.8$ m/s^2.

range of properties, consistent with a broad functional significance.

Role of NU in vestibular processing and the VOR

The nodulus has been strongly implicated in the processing of vestibular-related behaviours and has direct reciprocal connections with the VN (Precht *et al.* 1976; Kotchabhakdi & Walberg, 1978*a*,*b*; Carleton & Carpenter, 1984; Walberg & Dietrichs, 1988; Barmack *et al.* 1993; Naito *et al.* 1995; Ono *et al.* 2000; Xiong & Matsushita, 2000*a*,*b*; Purcell & Perachio, 2001; Barmack, 2003; Newlands *et al.* 2003). NU afferents originate from broad areas of the VN bilaterally (Brodal & Brodal, 1985; Epema *et al.* 1985; Sato *et al.* 1989; Thunnissen *et al.* 1989; Barmack *et al.* 1992*a*,*b*; Ono *et al.* 2000). NU afferents project in a topographic fashion back onto the VN, such that the lateral NU projects to the caudal medial VN and the medial NU to the middle part of medial VN (Shojaku *et al.* 1987; Wylie *et al.* 1994; Voogd *et al.* 1996; Fushiki & Barmack, 1997). There is evidence that electrical stimulation of the nodulus inhibits vestibulocerebellar pathways (Precht *et al.* 1976), suggesting that some of the NU-target neurons identified here might project back to the cerebellum.

NU Purkinje cells are not sensitive to eye movements, but exhibit strong responses to otolith system activation (Marini *et al.* 1975; Fushiki & Barmack, 1997; Yakusheva *et al.* 2007) and many otolith-activated VN cells project to the NU (Ono *et al.* 2000). Additionally, like VN neurons (Angelaki & Dickman, 2000; Dickman & Angelaki, 2002), many NU Purkinje cells in rabbits and mice respond to both activation of the vertical canals and the otolith system (Barmack & Shojaku, 1995; Fushiki & Barmack, 1997). More recently it was shown that NU Purkinje cells carry the output signals of an internal model that distinguishes heading direction (translation) and head orientation relative to gravity (tilt) using canal/otolith convergence (Yakusheva *et al.* 2007; Laurens *et al.*

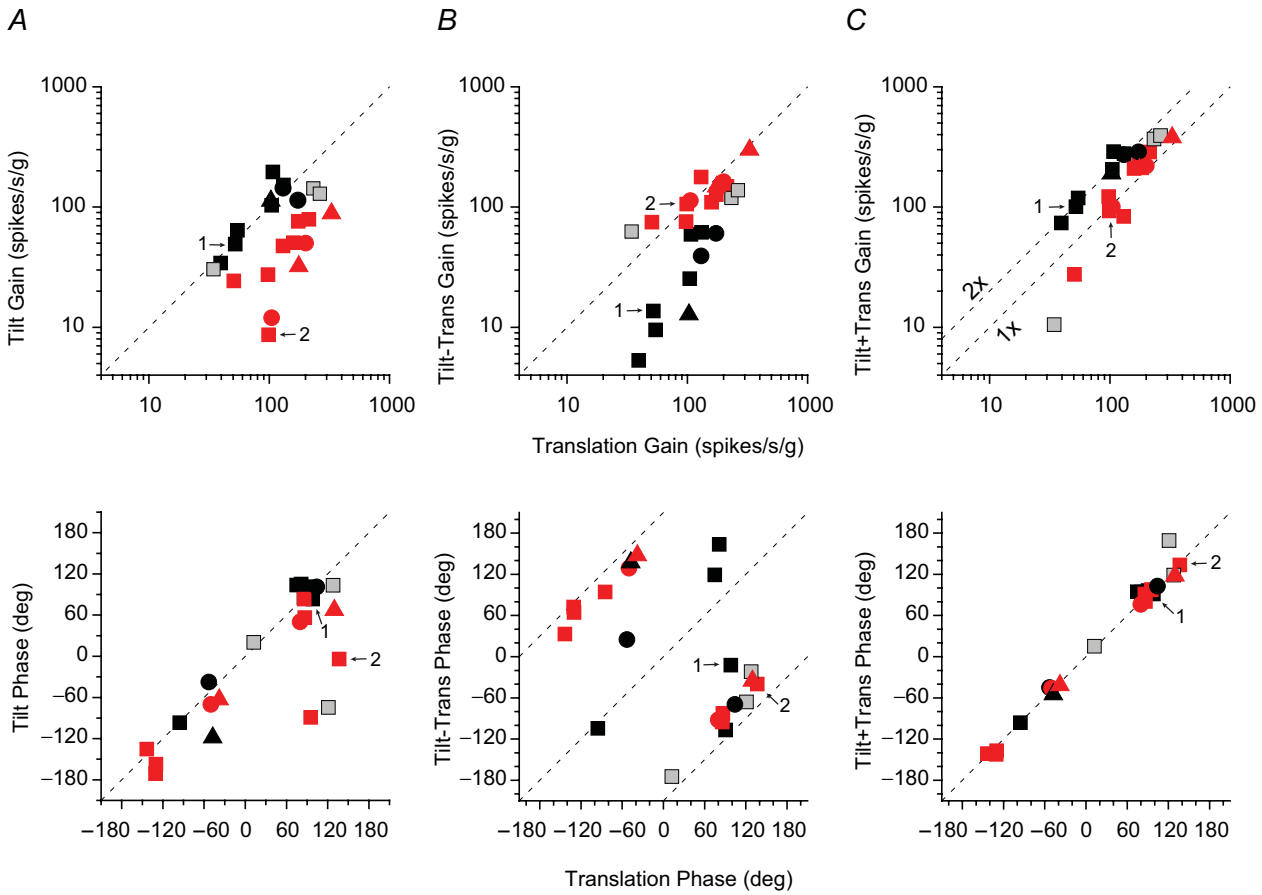

Figure 7. Summary of NU-target neuron responses during combinations of translation and tilt
Response gain (top row) and phase (bottom row) during tilt (*A*), tilt-translation (*B*) and tilt+translation (*C*) are plotted as a function of their respective responses during translation only motion (0.5 Hz). Red symbols indicate translation (TA)-coding cells, black symbols indicate net gravitoinertial acceleration (GIA)-coding cells and grey symbols indicate composite cells (see Methods for classification criteria). Different symbols represent data from different animals. Data points marked 1 and 2 denote the cells 1 and 2 from Fig. 6. $g = 9.8$ m/s^2.

2013*a*,*b*). Furthermore, stimulation and lesion studies have demonstrated a role of the NU in the canal/otolith interactions that govern the spatial organization of the low-frequency VOR (velocity storage; Cohen *et al.* 1992; Angelaki & Hess, 1995*a*,*b*; Wearne *et al.* 1998; Wiest *et al.* 1999; Barmack *et al.* 2002). For example, electrical stimulation of the NU results in shortening of the horizontal VOR time constant (Solomon & Cohen, 1994; Fig. 3) and NU ablation was found to compromise velocity storage properties in monkeys (Angelaki & Hess, 1995*a*,*b*; Wearne *et al.* 1998).

In agreement with previous studies (Solomon & Cohen, 1994), we show that electrical stimulation of the nodulus and ventral uvula does not generate nystagmus when delivered alone, but results in shortening of the horizontal VOR time constant. Electrical stimulation of the dorsal uvula results in nystagmus (with a rapid rise in eye velocity and no after-response) but does not change the horizontal VOR time constant (Heinen *et al.* 1992; Solomon & Cohen, 1994). Although electrode placement was not histologically verified in the present experiments, our results in terms of NU stimulation and the relative location

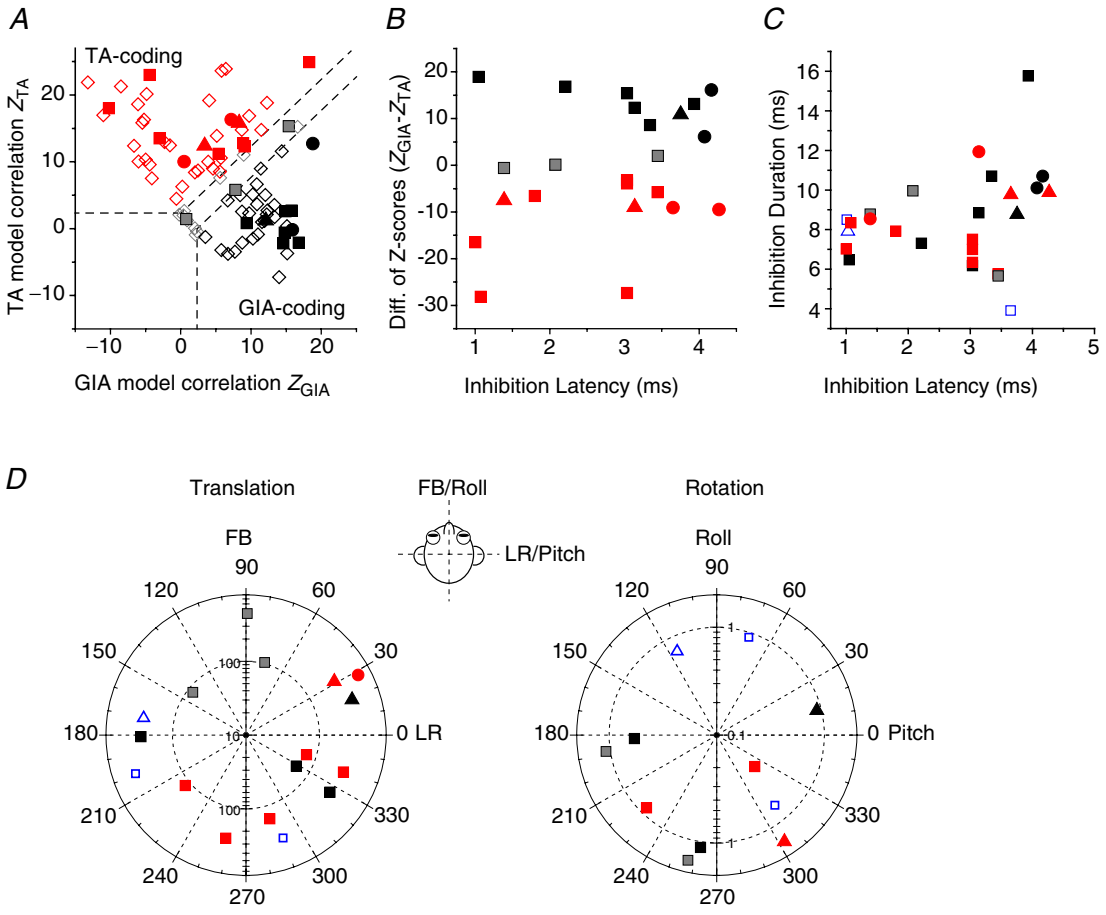

Figure 8. Summary of translation/rotation response properties of NU-target cells
A, scatter plot of *z*-scores, showing partial correlation coefficients for each cell's response fit with TA and GIA models. The superimposed dashed lines divide the plots into three regions: a top left area corresponding to cell responses with a significantly better fit ($P < 0.01$) by the TA model (red symbols), a bottom right area that includes neurons significantly better fit by the GIA model (black symbols) and an in-between area that includes cells not significantly better fit by either model (grey symbols). Filled symbols: NU-target cells. Open diamonds: VN data from Angelaki *et al.* (2004), shown for comparison. *B*, scatter plot of the difference in *z*-scores between the TA and GIA models ($Z_{GIA} - Z_{TA}$) *vs.* inhibition latency. *C*, scatter plot of inhibition duration *vs.* inhibition latency for non-EM cells colour-coded as in *A*. *D*, polar plots of preferred vector orientations (i.e. directions of maximum response gain) of NU-target neurons during horizontal plane translation (left) and vertical plane rotations (right), colour-coded as in *A*. The distance of each symbol from the centre indicates its gain (in units of spikes/s/g for translation and spikes/s/deg/s for rotation), whereas the angular position of each symbol corresponds to its preferred vector orientation (FB, forward–backward translation; LR, lateral translation). Blue open symbols in *C* and *D* indicate cells not tested with combinations of translation and rotation (thus not classified as TA- or GIA-selective). Different symbols represent data from different animals.

of sites that elicited nystagmus *versus* those that did not (e.g. Figs 1–3) were consistent with previous findings. Electrical stimulation in the NU would be the equivalent to a change in firing rate in output neurons (Purkinje cells), which could be understood by the system as a change in head orientation with respect to gravity and this would decrease the time constant of the rotational nystagmus (Waespe *et al.* 1985; Angelaki & Hess, 1994*a*, 1995*a*; Wearne *et al.* 1998).

Accurate inertial acceleration information is necessary to generate compensatory eye movements during translation (Angelaki *et al.* 1999) and the NU seems to be essential for that function. During translation the brainstem generates angular eye movements proportional to the translation of the head and scaled by the inverse of the viewing distance (see Angelaki & Hess, 2005 for a review). Perhaps one of the main roles of the NU is to provide eye-related and non-eye-related systems with an estimate of translation and tilt, which is used as input signals for further computations specific to each motor system. Thus, is it not surprising that NU-target neurons in the VN consist of both EM and non-EM neurons.

Diversity of non-EM NU-target neuron responses

Non-EM NU-target neurons were tested during combinations of tilt and translation to distinguish whether they selectively encode translation, tilt or net GIA. Previous studies have shown that VN neurons represent a continuum, with some cells being translation-selective, some tilt-selective, some GIA-selective and others with in-between properties (Angelaki *et al.* 2004; Shaikh *et al.* 2005; Zhou *et al.* 2006). In contrast, the majority of NU Purkinje cells selectively encode translation or tilt, whereas few are GIA-selective (Yakusheva *et al.* 2007, 2010; Laurens *et al.* 2013*a*,*b*). Unlike expectations given their connection with the NU, NU-target neurons in the VN were a mixture of translation-selective, GIA-selective and composite neurons, similar as the whole VN population (Angelaki *et al.* 2004). No tilt-selective neurons were observed, which could imply that there are no NU-target neurons that selectively respond to tilt. If this is indeed true, one would expect that lesions of the NU alter the VOR in response to translation but not in response to tilt, which would be in line with experimental findings (Walker *et al.* 2008, 2010; see also Angelaki & Hess, 1994*a*, 1995*a*,*b*). Although this possibility cannot be excluded, it is also possible that tilt-selective cells were missed. Although our lab has identified tilt-selective cells in the NU (Laurens *et al.* 2013*b*), we have never recorded from tilt VN neurons (but see Zhou *et al.* 2006).

NU-target cells were recorded from a broad area in the VN covering the rostral portion containing EM neurons to more caudal regions containing mainly non-EM cells. Although we tried to explore the VN bilaterally, NU-target neurons were found exclusively in the ipsilateral VN (relative to the stimulation electrode). These findings are in agreement with previous anatomical findings (Haines, 1977; Carleton & Carpenter, 1983).

Comparison between NU- and FL-target neurons

One might have expected that NU-target neurons are analogous to flocculus target neurons (FTNs) in the vestibular nuclei. Based on their physiological properties, FTNs form a uniform population characterized by a strong eye velocity signal during pursuit (Zhang *et al.* 1993, Lisberger *et al.* 1994). Using a combination of anatomical tracing and electrophysiological recordings in transgenic mouse lines, Shin *et al.* (2011) identified several classes of FTNs in the medial vestibular nucleus, including glycinergic, GABAergic and glutamatergic neurons. FTNs, many of which project to ocular motoneurons (Zhang *et al.* 1993; Shin *et al.* 2011), receive direct or indirect brainstem inputs from two opposite semicircular canal afferents (Blazquez *et al.* 2000; Broussard & Lisberger, 1992) and gaze velocity information from the cerebellar flocculus complex (i.e. flocculus and ventral paraflocculus, collectively referred to here as FL; Lisberger, 1994; Partsalis *et al.* 1995; Zhang *et al.* 1995). FTNs are generally thought of as gaze velocity neurons, whose response is dominated by their FL input (gaze velocity) while head velocity information from opposite semicircular canals tends to cancel each other (Lisberger, 1994; but see Zhang *et al.* 1995; Blazquez *et al.* 2000).

If the response of NU-target neurons were analogous to those of gaze velocity FTNs, we would expect them to be translation-sensitive, similar to NU Purkinje cells. However, our population of NU-target neurons showed a wide range of responses, suggesting that inputs arriving from sources other than the NU are not properly balanced; that is, they cancel each other at the level of NU-target neurons. A strong response during the linear translation paradigm is the only common response feature of the non-EM cells identified here as NU-target neurons.

There are some important anatomical differences between the NU–brainstem and the FL–brainstem circuitry. For example, the FL receives mostly indirect projections from vestibular afferents (Langer *et al.* 1985; Epema *et al.* 1990; Newlands *et al.* 2002; but see Newlands *et al.* 2003). In contrast, the NU receives more than 70% of ipsilateral vestibular afferents (including otolith organs and semicircular canals) as mossy fibres (Carpenter *et al.* 1972; Korte & Mugnaini, 1979; Kevetter & Perachio, 1986; Gerrits *et al.* 1989; Barmack *et al.* 1993; Newlands *et al.* 2002, 2003; Maklad & Fritzsch, 2003; Kevetter *et al.* 2004). Most FTNs are secondary vestibular neurons (Broussard & Lisberger, 1992; Zhang *et al.* 1995), while it is currently unknown whether NU-target neurons receive direct or

indirect projections from vestibular afferents. In addition, unlike the FL (De Zeeuw *et al.* 1994), NU Purkinje cell axons can contact a large diversity of target neurons in the vestibular and cerebellar nuclei (Wylie *et al.* 1994).

There is strong evidence to suggest that cerebellar and brainstem pathways to FTNs undergo plastic changes necessary for motor learning of the VOR (Lisberger, 1994; Blazquez *et al.* 2006, 2007). Cerebellar and brainstem pathways to NU-target neurons may also play a key role in vestibular-related adaptation, although no behavioural paradigms are currently available that allow modifications of the normal balance of input signals (e.g. canal and otolith) according to an error signal (visual or somatosensory). Learning in the NU–brainstem circuit would help compensate for developmental changes and cell death, and it would be essential to adapt astronauts to microgravity conditions.

Inhibition parameters

None of our recorded neurons was antidromically activated by NU stimulation, and thus the pause in firing rate was not the consequence of the refractory period of the neuron. NU-target neurons show a wide range of orthodromic latencies (∼1–4.5 ms), which, in many cases, were longer than 2.5 ms. Latency values of about 2.5 ms and below were reported for FL-target neurons in the VN (Lisberger *et al.* 1994: latency 0.8–2.2 ms, duration 3.3–24.9 ms; Zhang *et al.* 1993; 1995: latency 0.4–2.4 ms, duration 3.0–14.9 ms). As the same current intensity of 400 μA was applied to all sites in the present experiments, variations in inhibition duration and latency are probably due to different connection strengths and the characteristics of the pathways connecting the stimulation site with the recorded neuron. We suggest that NU-target neurons with long ortodromic latencies (>2.5 ms) are also NU-target neurons that are indirectly activated via parallel fibres; that is, electrical stimulation synchronously activates parallel fibres and generates a wave of excitation that activates Purkinje cells a few millimetres away. Using a value of 0.5 m/s for the conduction velocity at the parallel fibres and a synaptic delay of 0.3–0.5 ms (Eccles *et al.* 1966; Bernard & Axelrad, 1991), it would not be surprising to find latencies above 3.5 ms. The indirect activation effect may be more apparent in our experiments than in experiments characterizing FL-target neurons because of the comparatively larger size of the NU compared to the area containing gaze velocity Purkinje cells in the FL ($8 \times 4 \times 7$ mm^3 for NU; Fig. 1; *vs.* $4 \times 4 \times 7$ mm^3 for FL; Rambold *et al.* 2002).

Another explanation for the long latencies found in some NU-target neurons is indirect inhibition via the rostral fastigial nuclei (FN) (i.e. stimulation→Purkinje cells→FN→VN neurons), although only the most medial zone of the ventral nodulus projects to the FN and the white matter around both the fastigial and the anterior interposed nuclei (Wylie *et al.* 1994; Voogd *et al.* 1996). Longer latency inhibition might also be due to polysynaptic connections through other VN neurons. We found no relationship between the response properties of VN neurons and their orthodromic latency, although there was a non-significant tendency for translation-selective NU-target neurons to have smaller latencies (Fig. 8). Lastly, the pause in VN activity following NU stimulation could be a consequence of antidromic activation of other neurons in the VN and FN that indirectly contact (via inhibitory interneurons) with the recorded VN cell. This is probably an unlikely scenario because it would require a significant degree of convergence of antidromically activated neurons and their inhibitory target neurons into the recorded neurons.

Conclusions

In summary, NU-target neurons in the VN were found to be very diverse, in terms of both their eye movement and their vestibular response properties. NU-target neurons could respond to yaw rotation, translation, vertical plane rotation or any combination. We found that NU-target neurons were heterogeneous in their encoding of translation, GIA and in-between signals, similar to the representation within the VN (Angelaki *et al.* 2004). NU-target neurons were as likely to be afferent-like as they were to selectively respond to translation rather than net GIA. Notably, we never found tilt-selective neurons (Zhou *et al.* 2006) in the present study, although we have not searched the most caudal portions of the vestibular nuclei (Fig. 1). Thus, it is possible that the diversity of NU-target neurons is even larger than presented here.

References

Angelaki DE (1991). Dynamic polarization vector of spatially tuned neurons. *IEEE Trans Biomed Eng* **38**, 1053–1060.

Angelaki DE (1998). Three-dimensional organization of otolith-ocular reflexes in rhesus monkeys. III. Responses to translation. *J Neurophysiol* **80**, 680–695.

Angelaki DE & Dickman JD (2000). Spatiotemporal processing of linear acceleration: primary afferent and central vestibular neuron responses. *J Neurophysiol* **84**, 2113–2132.

Angelaki DE, Green AM & Dickman JD (2001). Differential sensorimotor processing of vestibulo-ocular signals during rotation and translation. *J Neurosci* **21**, 3968–3985.

Angelaki DE & Hess BJ (1994*a*). The cerebellar nodulus and ventral uvula control the torsional vestibulo-ocular reflex. *J Neurophysiol* **72**, 1443–1447.

Angelaki DE & Hess BJ (1994*b*). Inertial representation of angular motion in the vestibular system of rhesus monkeys. I. Vestibuloocular reflex. *J Neurophysiol* **71**, 1222–1249.

Angelaki DE & Hess BJ (1995*a*). Lesion of the nodulus and ventral uvula abolish steady-state off-vertical axis otolith response. *J Neurophysiol* **73**, 1716–1720.

Angelaki DE & Hess BJ (1995*b*). Inertial representation of angular motion in the vestibular system of rhesus monkeys. II. Otolith-controlled transformation that depends on an intact cerebellar nodulus. *J Neurophysiol* **73**, 1729–1751.

Angelaki DE & Hess BJM (2005). Self-motion-induced eye movements: effects on visual acuity and navigation. *Nat Rev Neurosci* **6**, 966–976.

Angelaki DE, McHenry MQ, Dickman JD, Newlands SD & Hess BJ (1999). Computation of inertial motion: neural strategies to resolve ambiguous otolith information. *J Neurosci* **19**, 316–327.

Angelaki DE, McHenry MQ & Hess BJ (2000). Primate translational vestibuloocular reflexes. I. High-frequency dynamics and three-dimensional properties during lateral motion. *J Neurophysiol* **83**, 1637–1647.

Angelaki DE, Shaikh AG, Green AM & Dickman JD (2004). Neurons compute internal models of the physical laws of motion. *Nature* **430**, 560–564.

Angelaki DE & Yakusheva TA (2009). How vestibular neurons solve the tilt/translation ambiguity. Comparison of brainstem, cerebellum, and thalamus. *Ann N Y Acad Sci* **1164**, 19–28.

Angelaki DE, Yakusheva TA, Green AM, Dickman JD & Blazquez PM (2010). Computation of egomotion in the macaque cerebellar vermis. *Cerebellum* **9**, 174–182.

Barmack NH (2003). Central vestibular system: vestibular nuclei and posterior cerebellum. *Brain Res Bull* **60**, 511–541.

Barmack NH, Baughman RW & Eckenstein FP (1992*a*). Cholinergic innervation of the cerebellum of rat, rabbit, cat, and monkey as revealed by choline acetyltransferase activity and immunohistochemistry. *J Comp Neurol* **317**, 233–249.

Barmack NH, Baughman RW, Eckenstein FP & Shojaku H (1992*b*). Secondary vestibular cholinergic projection to the cerebellum of rabbit and rat as revealed by choline acetyltransferase immunohistochemistry, retrograde and orthograde tracers. *J Comp Neurol* **317**, 250–270.

Barmack NH, Baughman RW, Errico P & Shojaku H (1993). Vestibular primary afferent projection to the cerebellum of the rabbit. *J Comp Neurol* **327**, 521–534.

Barmack NH, Errico P, Ferraresi A, Fushiki H, Pettorossi VE & Yakhnitsa V (2002). Cerebellar nodulectomy impairs spatial memory of vestibular and optokinetic stimulation in rabbits. *J Neurophysiol* **87**, 962–975.

Barmack NH & Shojaku H (1995). Vestibular and visual climbing fibre signals evoked in the uvula-nodulus of the rabbit cerebellum by natural stimulation. *J Neurophysiol* **74**, 2573–2589.

Barmack NH & Yakhnitsa V (2002). Vestibularly evoked climbing-fibre responses modulate simple spikes in rabbit cerebellar Purkinje neurons. *Ann N Y Acad Sci* **978**, 237–254.

Barmack NH & Yakhnitsa V (2003). Cerebellar climbing fibers modulate simple spikes in Purkinje cells. *J Neurosci* **23**, 7904–7916.

Bernard C & Axelrad H (1991). Propagation of parallel fibre volleys in the cerebellar cortex: a computer simulation. *Brain Res* **565**, 195–208.

Blazquez P, Partsalis A, Gerrits NM & Highstein SM (2000). Input of anterior and posterior semicircular canal interneurons encoding head-velocity to the dorsal Y group of the vestibular nuclei. *J Neurophysiol* **83**, 2891–2904.

Blazquez PM, Davis-Lopez de Carrizosa MA, Heiney SA & Highstein SM (2007). Neuronal substrates of motor learning in the velocity storage generated during optokinetic stimulation in the squirrel monkey. *J Neurophysiol* **97**, 1114–1126.

Blazquez PM, Hirata Y & Highstein SM (2006). Chronic changes in inputs to dorsal Y neurons accompany VOR motor learning. *J Neurophysiol* **95**, 1812–1825.

Boyden ES, Katoh A & Raymond JL (2004). Cerebellum-dependent learning: the role of multiple plasticity mechanisms. *Annu Rev Neurosci* **27**, 581–609.

Brodal A & Brodal P (1985). Observations on the secondary vestibulocerebellar projections in the macaque monkey. *Exp Brain Res* **58**, 62–74.

Broussard DM & Lisberger SG (1992). Vestibular inputs to brain stem neurons that participate in motor learning in the primate vestibuloocular reflex. *J Neurophysiol* **68**, 1906–1909.

Broussard DM, Titley HK, Antflick J & Hampson DR (2011). Motor learning in the VOR: the cerebellar component. *Exp Brain Res* **210**, 451–463.

Bush GA, Perachio AA & Angelaki DE (1993). Encoding of head acceleration in vestibular neurons. I. Spatiotemporal response properties to linear acceleration. *J Neurophysiol* **69**, 2039–2055.

Carleton SC & Carpenter MB (1983). Afferent and efferent connections of the medial, inferior and lateral vestibular nuclei in the cat and monkey. *Brain Res* **278**, 29–51.

Carleton SC & Carpenter MB (1984). Distribution of primary vestibular fibers in the brainstem and cerebellum of the monkey. *Brain Res* **294**, 281–298.

Carpenter MB, Stein BM & Peter P (1972). Primary vestibulocerebellar fibers in the monkey: distribution of fibers arising from distinctive cell groups of the vestibular ganglia. *Am J Anat* **135**, 221–249.

Chen-Huang C & Peterson BW (2006). Three dimensional spatial-temporal convergence of otolith related signals in vestibular only neurons in squirrel monkeys. *Exp Brain Res* **168**, 410–426.

Chen-Huang C & Peterson BW (2010). Frequency-dependent spatiotemporal tuning properties of non-eye movement related vestibular neurons to three-dimensional translations in squirrel monkeys. *J Neurophysiol* **103**, 3219–3237.

Cohen B, Wearne S, Dai M & Raphan T (1999). Spatial orientation of the angular vestibulo-ocular reflex. *J Vestib Res* **9**, 163–172.

Cohen H, Cohen B, Raphan T & Waespe W (1992). Habituation and adaptation of the vestibuloocular reflex: a model of differential control by the vestibulocerebellum. *Exp Brain Res* **90**, 526–538.

De Zeeuw CI, Wylie DR, DiGiorgi PL, Simpson JI (1994). Projections of individual Purkinje cells of identified zones in the flocculus to the vestibular and cerebellar nuclei in the rabbit. *J Comp Neurol* **349**, 428–447.

Dickman JD & Angelaki DE (2002). Vestibular convergence patterns in vestibular nuclei neurons of alert primates. *J Neurophysiol* **88**, 3518–3533.

Dickman JD, Angelaki DE & Correia MJ (1991). Response properties of gerbil otolith afferents to small angle pitch and roll tilts. *Brain Res* **556**, 303–310.

Eccles JC, Llinás R & Sasaki K (1966). Parallel fibre stimulation and the responses induced thereby in the Purkinje cells of the cerebellum. *Exp Brain Res* **1**, 17–39.

Epema AH, Gerrits NM & Voogd J (1990). Secondary vestibulocerebellar projections to the flocculus and uvulo-nodular lobule of the rabbit: a study using HRP and double fluorescent tracer techniques. *Exp Brain Res* **80**, 72–82.

Epema AH, Guldemond JM & Voogd J (1985). Reciprocal connections between the caudal vermis and the vestibular nuclei in the rabbit. *Neurosci Lett* **57**, 273–278.

Fernández C & Goldberg JM (1976). Physiology of peripheral neurons innervating otolith organs of the squirrel monkey. I. Response to static tilts and to long-duration centrifugal force. *J Neurophysiol* **39**, 970–984.

Fernandez C, Goldberg JM & Abend WK (1972). Response to static tilts of peripheral neurons innervating otolith organs of the squirrel monkey. *J Neurophysiol* **35**, 978–987.

Fushiki H & Barmack NH (1997). Topography and reciprocal activity of cerebellar Purkinje cells in the uvula-nodulus modulated by vestibular stimulation. *J Neurophysiol* **78**, 3083–3094.

Gao Z, van Beugen BJ & De Zeeuw CI (2012). Distributed synergistic plasticity and cerebellar learning. *Nat Rev Neurosci* **13**, 619–635.

Gerrits NM, Epema AH, van Linge A & Dalm E (1989). The primary vestibulocerebellar projection in the rabbit: absence of primary afferents in the flocculus. *Neurosci Lett* **105**, 27–33.

Glasauer S & Mittelstaedt H (1997). Perception of spatial orientation in different g-levels. *J Gravit Physiol* **4**, P5–8.

Green AM & Angelaki DE (2004). An integrative neural network for detecting inertial motion and head orientation. *J Neurophysiol* **92**, 905–925.

Green AM & Angelaki DE (2007). Coordinate transformations and sensory integration in the detection of spatial orientation and self-motion: from models to experiments. *Prog Brain Res* **165**, 155–180.

Green AM, Meng H & Angelaki DE (2007). A reevaluation of the inverse dynamic model for eye movements. *J Neurosci* **27**, 1346–1355.

Green AM, Shaikh AG & Angelaki DE (2005). Sensory vestibular contributions to constructing internal models of self-motion. *J Neural Eng* **2**, S164–179.

Haines DE (1977). Cerebellar corticonuclear and corticovestibular fibers of the flocculonodular lobe in a prosimian primate (*Galago senegalensis*). *J Comp Neurol* **174**, 607–630.

Heinen SJ, Oh DK & Keller EL (1992). Characteristics of nystagmus evoked by electrical stimulation of the uvular/nodular lobules of the cerebellum in monkey. *J Vestib Res* **2**, 235–245.

Ilg UJ & Thier P (2008). The neural basis of smooth pursuit eye movements in the rhesus monkey brain. *Brain Cogn* **68**, 229–240.

Kevetter GA, Leonard RB, Newlands SD & Perachio AA (2004). Central distribution of vestibular afferents that innervate the anterior or lateral semicircular canal in the mongolian gerbil. *J Vestib Res* **14**, 1–15.

Kevetter GA & Perachio AA (1986). Distribution of vestibular afferents that innervate the sacculus and posterior canal in the gerbil. *J Comp Neurol* **254**, 410–424.

Korte GE & Mugnaini E (1979). The cerebellar projection of the vestibular nerve in the cat. *J Comp Neurol* **184**, 265–277.

Kotchabhakdi N & Walberg F (1978*a*). Primary vestibular afferent projections to the cerebellum as demonstrated by retrograde axonal transport of horseradish peroxidase. *Brain Res* **142**, 142–146.

Kotchabhakdi N & Walberg F (1978*b*). Cerebellar afferent projections from the vestibular nuclei in the cat: an experimental study with the method of retrograde axonal transport of horseradish peroxidase. *Exp Brain Res* **31**, 591–604.

Langer T, Fuchs AF, Scudder CA & Chubb MC (1985). Afferents to the flocculus of the cerebellum in the rhesus macaque as revealed by retrograde transport of horseradish peroxidase. *J Comp Neurol* **235**, 1–25.

Laurens J & Angelaki DE (2011). The functional significance of velocity storage and its dependence on gravity. *Exp Brain Res* **210**, 407–422.

Laurens J & Droulez J (2007). Bayesian processing of vestibular information. *Biol Cybern* **96**, 389–404.

Laurens J, Meng H & Angelaki DE (2013*a*). Computation of linear acceleration through an internal model in the macaque cerebellum. *Nature Neurosci* **16**, 1701–1708.

Laurens J, Meng H & Angelaki DE (2013*b*). Neural representation of orientation relative to gravity in the macaque cerebellum. *Neuron* (in press).

Lisberger SG (1994). Neural basis for motor learning in the vestibuloocular reflex of primates. III. Computational and behavioral analysis of the sites of learning. *J Neurophysiol* **72**, 974–998.

Lisberger SG (2009). Internal models of eye movement in the floccular complex of the monkey cerebellum. *Neuroscience* **162**, 763–776.

Lisberger SG (2010). Visual guidance of smooth-pursuit eye movements: sensation, action, and what happens in between. *Neuron* **66**, 477–491.

Lisberger SG, Pavelko TA & Broussard DM (1994). Responses during eye movements of brain stem neurons that receive monosynaptic inhibition from the flocculus and ventral paraflocculus in monkeys. *J Neurophysiol* **72**, 909–927.

Maklad A & Fritzsch B (2003). Partial segregation of posterior crista and saccular fibers to the nodulus and uvula of the cerebellum in mice, and its development. *Brain Res Dev Brain Res* **140**, 223–236.

Marini G, Provini L & Rosina A (1975). Macular input to the cerebellar nodulus. *Brain Res* **99**, 367–371.

Marini G, Provini L & Rosina A (1976). Gravity responses of Purkinje cells in the nodulus. *Exp Brain Res* **24**, 311–323.

Marlinski V & McCrea RA (2009). Self-motion signals in vestibular nuclei neurons projecting to the thalamus in the alert squirrel monkey. *J Neurophysiol* **101**, 1730–1741.

Meng H & Angelaki DE (2006). Neural correlates of the dependence of compensatory eye movements during translation on target distance and eccentricity. *J Neurophysiol* **95**, 2530–2540.

Meng H, Green AM, Dickman JD & Angelaki DE (2005). Pursuit–vestibular interactions in brain stem neurons during rotation and translation. *J Neurophysiol* **93**, 3418–3433.

Meng H, May PJ, Dickman JD & Angelaki DE (2007). Vestibular signals in primate thalamus: properties and origins. *J Neurosci* **27**, 13590–13602.

Merfeld DM (1995). Modeling human vestibular responses during eccentric rotation and off vertical axis rotation. *Acta Otolaryngol Suppl* **520**, 354–359.

Naito Y, Newman A, Lee WS, Beykirch K & Honrubia V (1995). Projections of the individual vestibular end-organs in the brain stem of the squirrel monkey. *Hear Res* **87**, 141–155.

Newlands SD, Purcell IM, Kevetter GA & Perachio AA (2002). Central projections of the utricular nerve in the gerbil. *J Comp Neurol* **452**, 11–23.

Newlands SD, Vrabec JT, Purcell IM, Stewart CM, Zimmerman BE & Perachio AA (2003). Central projections of the saccular and utricular nerves in macaques. *J Comp Neurol* **466**, 31–47.

Ono S, Kushiro K, Zakir M, Meng H, Sato H & Uchino Y (2000). Properties of utricular and saccular nerve-activated vestibulocerebellar neurons in cats. *Exp Brain Res* **134**, 1–8.

Partsalis AM, Zhang Y & Highstein SM (1995). Dorsal Y group in the squirrel monkey. II. Contribution of the cerebellar flocculus to neuronal responses in normal and adapted animals. *J Neurophysiol* **73**, 632–650.

Paul K & Gnadt JW (2003). Reliable real-time spike discrimination during microstimulation. *J Neurosci Methods* **128**, 191–195.

Precht W, Simpson JI & Llinás R (1976). Responses of Purkinje cells in rabbit nodulus and uvula to natural vestibular and visual stimuli. *Pflügers Arch* **367**, 1–6.

Purcell IM & Perachio AA (2001). Peripheral patterns of terminal innervation of vestibular primary afferent neurons projecting to the vestibulocerebellum in the gerbil. *J Comp Neurol* **433**, 48–61.

Rambold H, Churchland A, Selig Y, Jasmin L & Lisberger SG (2002). Partial ablations of the flocculus and ventral paraflocculus in monkeys cause linked deficits in smooth pursuit eye movements and adaptive modification of the VOR. *J Neurophysiol* **87**, 912–924.

Rota E, Morelli N, Immovilli P, Magnifico F, Crisi G & Guidetti D (2012). Acquired pendular nystagmus from cerebellar nodulus acute ischemic lesion. *Neurology* **79**, 832.

Sato Y, Kanda K, Ikarashi K & Kawasaki T (1989). Differential mossy fibre projections to the dorsal and ventral uvula in the cat. *J Comp Neurol* **279**, 149–164.

Shaikh AG, Green AM, Ghasia FF, Newlands SD, Dickman JD & Angelaki DE (2005). Sensory convergence solves a motion ambiguity problem. *Curr Biol* **15**, 1657–1662.

Shin M, Moghadam SH, Sekirnjak C, Bagnall MW, Kolkman KE, Jacobs R, Faulstich M, du Lac S (2011). Multiple types of cerebellar target neurons and their circuitry in the vestibulo-ocular reflex. *J Neurosci* **31**, 10776–10786.

Shojaku H, Sato Y, Ikarashi K & Kawasaki T (1987). Topographical distribution of Purkinje cells in the uvula and the nodulus projecting to the vestibular nuclei in cats. *Brain Res* **416**, 100–112.

Solomon D & Cohen B (1994). Stimulation of the nodulus and uvula discharges velocity storage in the vestibulo-ocular reflex. *Exp Brain Res* **102**, 57–68.

Thunnissen IE, Epema AH & Gerrits NM (1989). Secondary vestibulocerebellar mossy fibre projection to the caudal vermis in the rabbit. *J Comp Neurol* **290**, 262–277.

Voogd J, Gerrits NM & Ruigrok TJ (1996). Organization of the vestibulocerebellum. *Ann N Y Acad Sci* **781**, 553–579.

Waespe W, Cohen B & Raphan T (1985). Dynamic modification of the vestibulo-ocular reflex by the nodulus and uvula. *Science* **228**, 199–202.

Walberg F & Dietrichs E (1988). The interconnection between the vestibular nuclei and the nodulus: a study of reciprocity. *Brain Res* **449**, 47–53.

Walker MF, Tian J, Shan X, Tamargo RJ, Ying H & Zee DS (2008). Lesions of the cerebellar nodulus and uvula in monkeys: effect on otolith-ocular reflexes. *Prog Brain Res* **171**, 167–172.

Walker MF, Tian J, Shan X, Tamargo RJ, Ying H & Zee DS (2010). The cerebellar nodulus/uvula integrates otolith signals for the translational vestibulo-ocular reflex. *PLoS One* **5**, e13981.

Wearne S, Raphan T & Cohen B (1998). Control of spatial orientation of the angular vestibuloocular reflex by the nodulus and uvula. *J Neurophysiol* **79**, 2690–2715.

Wearne S, Raphan T, Waespe W & Cohen B (1997). Control of the three-dimensional dynamic characteristics of the angular vestibulo-ocular reflex by the nodulus and uvula. *Prog Brain Res* **114**, 321–334.

Wiest G, Deecke L, Trattnig S & Mueller C (1999). Abolished tilt suppression of the vestibulo-ocular reflex caused by a selective uvulo-nodular lesion. *Neurology* **52**, 417–419.

Wylie DR, De Zeeuw CI, DiGiorgi PL & Simpson JI (1994). Projections of individual Purkinje cells of identified zones in the ventral nodulus to the vestibular and cerebellar nuclei in the rabbit. *J Comp Neurol* **349**, 448–463.

Xiong G & Matsushita M (2000*a*). Connections of Purkinje cell axons of lobule X with vestibulospinal neurons projecting to the cervical cord in the rat. *Exp Brain Res* **131**, 491–499.

Xiong G & Matsushita M (2000*b*). Connections of Purkinje cell axons of lobule X with vestibulocerebellar neurons projecting to lobule X or IX in the rat. *Exp Brain Res* **133**, 219–228.

Yakhnitsa V & Barmack NH (2006). Antiphasic Purkinje cell responses in mouse uvula-nodulus are sensitive to static roll-tilt and topographically organized. *Neuroscience* **143**, 615–626.

Yakusheva T, Blazquez PM & Angelaki DE (2008). Frequency-selective coding of translation and tilt in macaque cerebellar nodulus and uvula. *J Neurosci* **28**, 9997–10009.

Yakusheva T, Blazquez PM & Angelaki DE (2010). Relationship between complex and simple spike activity in macaque caudal vermis during three-dimensional vestibular stimulation. *J Neurosci* **30**, 8111–8126.

Yakusheva TA, Shaikh AG, Green AM, Blazquez PM, Dickman JD & Angelaki DE (2007). Purkinje cells in posterior cerebellar vermis encode motion in an inertial reference frame. *Neuron* **54**, 973–985.

Zhang Y, Partsalis AM & Highstein SM (1993). Properties of superior vestibular nucleus neurons projecting to the cerebellar flocculus in the squirrel monkey. *J Neurophysiol* **69**, 642–645.

Zhang Y, Partsalis AM & Highstein SM (1995). Properties of superior vestibular nucleus flocculus target neurons in the squirrel monkey. I. General properties in comparison with flocculus projecting neurons. *J Neurophysiol* **73**, 2261–2278.

Zhou W, Tang BF, Newlands SD & King WM (2006). Responses of monkey vestibular-only neurons to translation and angular rotation. *J Neurophysiol* **96**, 2915–2930.

Zupan LH, Merfeld DM & Darlot C (2002). Using sensory weighting to model the influence of canal, otolith and visual cues on spatial orientation and eye movements. *Biol Cybern* **86**, 209–230.

Additional information

Competing interests

There are no conflict of interests.

Author contributions

H.M. designed experiments, performed experiments and data analysis, and prepared the manuscript. P.M.B. participated in experiments and data analysis and prepared the manuscript. J.D.D. participated in experiments and prepared the manuscript. D.E.A. supervised all aspects of the work, designed experiments and prepared the manuscript.

Funding

The study was supported by a National Institutes of Health grant (RO1- EY12814) to D.E.A.

Acknowledgements

We thank Dr E. Klier for helping with the writing, Jean Laurens for helping with the analysis scripts, and Turner and Jing Lin for excellent technical assistance.